Available online at www.scholarsresearchlibrary.com

Scholars Research Library

Der Pharmacia Lettre, 2016, 8 (4):151-160
(http://scholarsresearchlibrary.com/archive.html)

ISSN 0975-5071
USA CODEN: DPLEB4

Electronic structure and reactivity analysis of some TTF-donor substituted molecules

Amel Bendjeddou[1*], Tahar Abbaz[1,3], Rachida Khammar[1], Rabah Rehamnia[2], Abdelkrim Gouasmia[3] and Didier Villemin[4]

[1]*Laboratory of Aquatic and Terrestrial Ecosystems, Organic and Bioorganic Chemistry group, University of Mohamed-Cherif Messaadia, Souk Ahras, Algeria*
[2]*Chemistry Department, Faculty of Science, University of badji mokhtar, Annaba, Algeria*
[3]*Laboratory of Organic Materials and Heterochemistry, University of Larbi Tebessi, Tebessa, Algeria*
[4]*Laboratory of Molecular and Thio-Organic Chemistry, UMR CNRS 6507, INC3M, FR 3038, Labex EMC3, ensicaen & University of Caen, Caen 14050, France*

ABSTRACT

In the present work a number of reactivity descriptors such as (E_{HOMO}), (E_{LUMO}) energy gap (ΔE_{gap}), hardness (η), softness (S) and electronegativity (χ) of some TTF-donor substituted molecules were investigated with the density functional theory DFT employing the 6-31G(d,p) basis sets in an attempt to elucidate their chemical reactivity. Fukui index has also employed to determine the reactivity of each atom in the molecule in order to predict reactive sites on the molecule for nucleophilic, electrophilic and radical attacks. The chemometric methods PCA and HCA were employed to find the subset of variables that could correctly classify the compounds according to their reactivity.

Keywords: Tetrathiafulvalenes, Density Functional Theory, Reactivity descriptors, Principal Component Analysis and Hierarchical Cluster Analysis

---

INTRODUCTION

The synthesis and characterization of new heterocyclic systems based on chalcogens (oxygen, sulfur, selenium and tellurium) has been one of the central objectives in contemporary organic chemistry. Several interesting systems have been synthesized and characterized. Especially, sulfur-based heterocyclic systems have found widespread applications in modern material science and medicinal chemistry [1]. Tetrathiafulvalenes and related heterocycles have received much interest due to their unique electron-donating capabilities [2]. A number of interesting properties of the TTF moiety includes its ability to form molecular metals and superconductors at low temperatures. It has also been incorporated in a number of macrocyclic systems for use as molecular sensors, enzyme biosensors, switches, wires and shuttles, exploiting the inherent electron donor properties [3].

The main purposes of theoretical chemistry based on the adequate knowledge of the general behavior of a molecular system and also to predict the reactivity of atoms and molecules as well as site selectivity [4-6]. Density functional theory [5,7] has been quite successful approximate method for many body systems, especially in the field of organic chemistry. During the last decades, density functional theory (DFT) has undergone fast development, especially in the field of organic chemistry, as the number of accurate exchange–correlation functionals increased. Indeed, the apparition of gradient corrected and hybrid functionals in the late 1980s greatly improved the chemical accuracy of the Hohenberg-Kohn theorem [8] based methods. The Kohn–Sham formalism [9] and its density-derived orbitals paved the way to computational methods. In parallel, a new field of application of DFT developed, the so-called

conceptual DFT [7]. Parr and Yang followed the idea that well-known chemical properties as electronegativity, chemical potentials and affinities could be sharply described and calculated manipulating the electronic density as the fundamental quantity [10,5]. Moreover, starting from the work of Fukui and its frontier molecular orbitals (FMOs) theory [11], the same authors further generalized the concept and proposed the Fukui function as a tool for describing the local reactivity in molecules [12,13]. In the present work an attempt has been made to explore the uses of DFT descriptors for some TTF-donor substituted molecules in order to understand their interaction mechanism and to elucidate the centres in the compounds on which such interactions are likely to occur**.**

MATERIALS AND MEHTODS

All computational calculations have been performed on personal computer using the Gaussian 09W program packages developed by Frisch and coworkers. [14] The Becke's three parameter hybrid functional using the LYP correlation functional (B3LYP), one of the most robust functional of the hybrid family, was herein used for all the calculations, with 6.31G (d, p) basis set. [15,16] Gaussian output files were visualized by means of GAUSSIAN VIEW 05 software. [17] Principal component analysis (PCA) [18,19] is a chemometric method was performed using software XLSTAT.

RESULTS AND DISCUSSION

In a previous work [20], we have described the synthesis of TTF-donor substituted molecules (**2-4**) indicated in Scheme 1. The strategies toward the TTF-dimethylaniline (TTF-DMA) **4** are based on an organometallic cross-coupling reaction between a tributylstannyl-TTF derivative and a *p*-halogeno-aromatic compound (route a). A multistep procedure (route c) was envisioned, offering much better overall yields (44 - 50%) from the appropriate tributylstannyl-TTF derivatives **1b** and **1c**, and the *p*-nitrobenzene as a reagent. In this case, the strong electron-withdrawing nitro group increased the reactivity of the Stille reaction, and the donor - acceptor entities **2b** (R = R′ = CH_3) and **2c** (R = CH_3, R′ = H) were isolated in very high yields (98 and 96%, respectively). In the second step of the synthetic process the nitro derivatives **2** were reduced into the corresponding amino compounds **3** in quite good yields (**3b**: 62%; **3c**: 65%). Finally the amino species **3** were successfully converted (74 - 78%) into the target N,N-dimethylated molecules **4** by a classical dialkylation reaction using an excess of dimethyliodide in a basic medium. Finally, a Suzuki cross-coupling reaction between the iodotetrathiafulvalene **1′** and the *p*-(dimethyl-amino) phenylboronic acid was then used (route b), leading to a modest improvement of the yield (22%).

Scheme 1. Synthetic route for the preparation of TTF-donor substituted molecules (2-4)

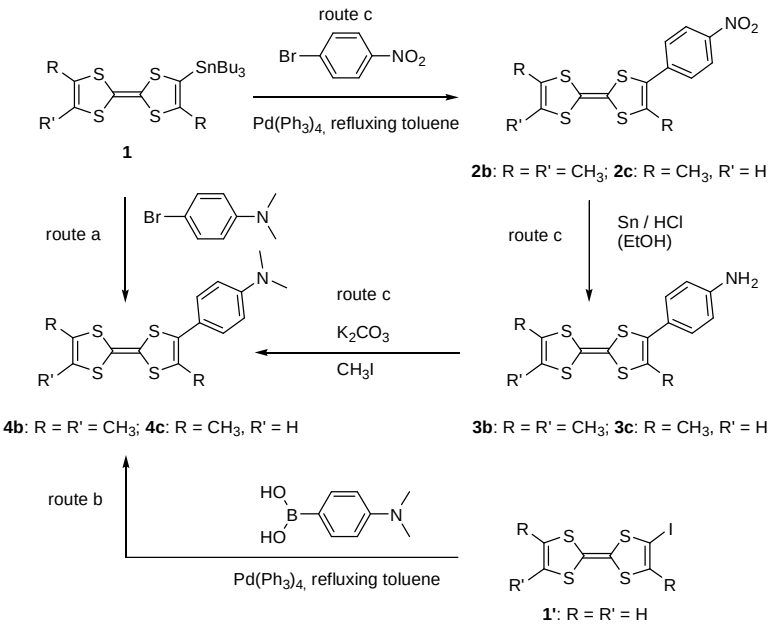

Molecular geometry

The molecular geometry analysis plays a very important role in determining the structure-reactivity relationship [21]. The molecular geometry can be described by the positions of atoms in space, evoking bond lengths of two joined atoms and bond angles of three connected atoms. The molecular geometries can be determined by the quantum mechanical behavior of the electrons and computed by *ab-initio* quantum chemistry methods to high

accuracy. Molecular geometry represents the three dimensional arrangement of the atoms that determines several properties of a substance including its reactivity, polarity, phase of matter, color, magnetism, and biological activity [22,23]. The optimization of the geometry for the molecules (**2-4**) has been achieved by energy minimization, using DFT at the B3LYP level, employing the basis set 6-31G(d,p).The following figure 1 and tables 1-3 represent the schemes of the optimized molecules, their bond lengths and their angle measurement.

Figure 1. Optimized molecular structure of TTF-donor substituted molecules (2-4)

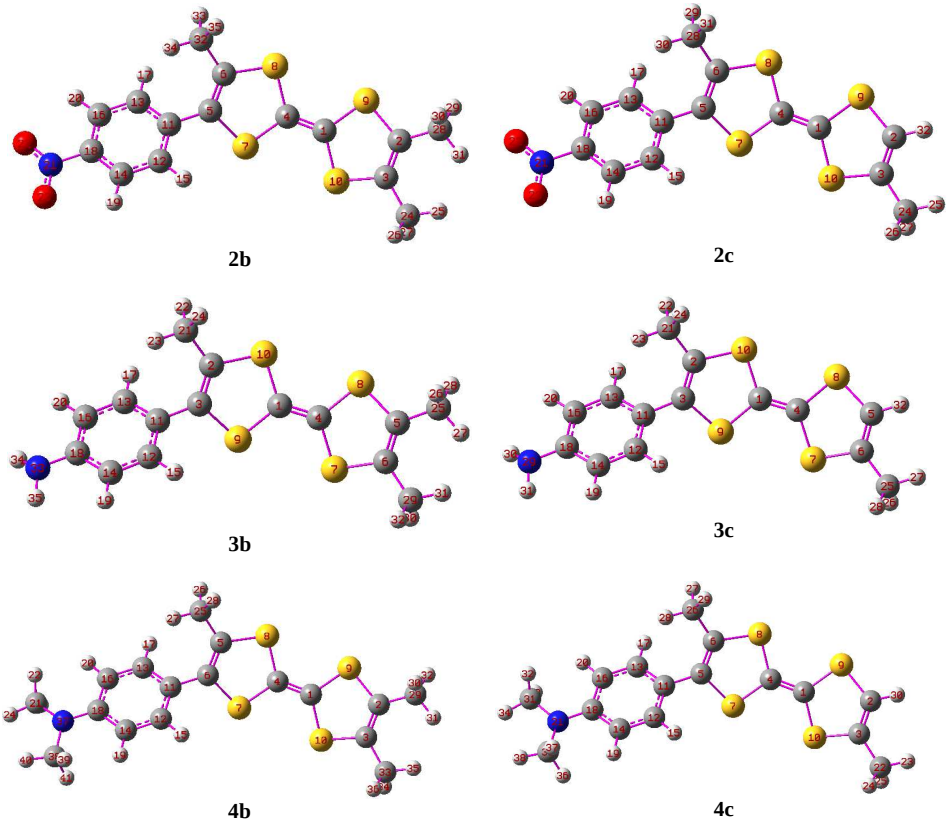

2b **2c**

3b **3c**

4b **4c**

Table 1: Optimized geometric parameters of compound (2b) and (2c)

Compound 2b				Compound 2c			
Bond length(Å)		**Bond Angles (°)**		**Bond length(Å)**		**Bond Angles (°)**	
1C2C	1.35	4C1C9S	123.55	1C4C	1.35	4C1C9S	123.33
1C9S	1.78	1C9S2C	95.65	1C9S	1.78	1C9S2C	94.56
9S2C	1.78	9S2C3C	116.99	9S2C	1.76	9S2C3C	119.22
2C3C	1.34	9S2C28C	115.01	2C3C	1.34	32H2C3C	124.07
2C28C	1.50	28C2C3C	127.98	2C32H	1.08	7S5C11C	116.07
11C13C	1.41	5C11C12C	120.47	2C24C	1.50	5C11C12C	120.68
5C11C	1.47	2C28C31H	111.38	5C11C	1.47	11C12C15H	119.43
18C21N	1.47	11C12C14C	121.01	11C12C	1.40	14C18C21N	119.14
21N22O	1.23	14C18C21N	119.14	18C21N	1.47	18C21N23O	117.66
28C31H	1.09	18C21N23O	117.67	21N23O	1.23	23O21N22O	124.67

Table 2: Optimized geometric parameters of compound (3b) and (3c)

Compound 3b				Compound 3c			
Bond length(Å)		**Bond Angles (°)**		**Bond length(Å)**		**Bond Angles (°)**	
1C4C	1.35	1C4C8S	123.61	1C4C	1.35	1C4C8S	123.39
4C2S	1.78	4C8S5C	95.54	4C8S	1.79	4C8S5C	94.49
8S5C	1.78	8S5C6C	117.01	8S5C	1.76	8S5C32H	116.77
5C6C	1.34	6C5C25C	127.92	5C6C	1.34	5C6C25C	126.44
25C27H	1.09	9S3C11C	115.89	5C32H	1.08	25C6C7S	117.49
3C11C	1.47	3C11C12C	121.08	6C25C	1.50	9S3C11C	115.89
5C25C	1.52	5C25C27H	111.42	3C11C	1.48	2C3C11C	127.48
11C12C	1.41	14C18C33N	120.86	11C12C	1.41	3C11C12C	121.08
18C33N	1.39	18C33N35H	115.58	18C29N	1.39	18C29N31H	115.61
33N35H	1.01	35H33N34H	112.23	29N31H	1.01	31H29N30H	112.26

Table 3: Optimized geometric parameters of compound (4b) and (4c)

Compound 4b				Compound 4c			
Bond length(Å)		**Bond Angles (°)**		**Bond length(Å)**		**Bond Angles (°)**	
1C4C	1.35	4C1C9S	123.60	1C4C	1.35	4C1C9S	123.37
1C9S	1.78	1C9S2C	95.55	1C9S	1.79	1C9S2C	94.51
9S2C	1.78	9S2C3C	117.01	9S2C	1.76	9S2C3C	119.22
2C3C	1.34	9S2C29C	115.05	2C3C	1.34	11C5C7S	115.84
6C11C	1.48	7S6C11C	115.88	3C22C	1.50	9S2C30H	116.77
2C29C	1.50	2C29C31H	111.47	2C30H	1.08	3C22C24H	111.44
29C31H	1.09	6C11C13C	121.63	5C11C	1.48	5C11C13C	121.60
11C13C	1.40	14C18C37N	121.48	11C13C	1.40	21N18C14C	121.48
18C37N	1.39	18C37N21C	119.45	18C21N	1.39	31C21N18C	119.63
37N21C	1.45	21C37N38C	118.24	21N31C	1.45	31C21N35C	118.77

Molecular electrostatic potential (ESP) map

Electrostatic potential maps, also known as electrostatic potential energy maps, or molecular electrical potential surfaces, illustrate the charge distributions of molecules three dimensionally. The purpose of finding the electrostatic potential is to find the reactive site of a molecule. These maps allow us to visualize variably charged regions of a molecule. Knowledge of the charge distributions can be used to determine how molecules interact with one another. Molecular electrostatic potential (MESP) mapping is very useful in the investigation of the molecular structure with its physiochemical property relationships [24]. Total SCF electron density surface mapped with molecular electrostatic potential (MESP) of compounds (**2b**) and (**4c**) are shown in Fig. 2.

Figure 2. Molecular electrostatic potential surface of compounds (2b) and (4c)

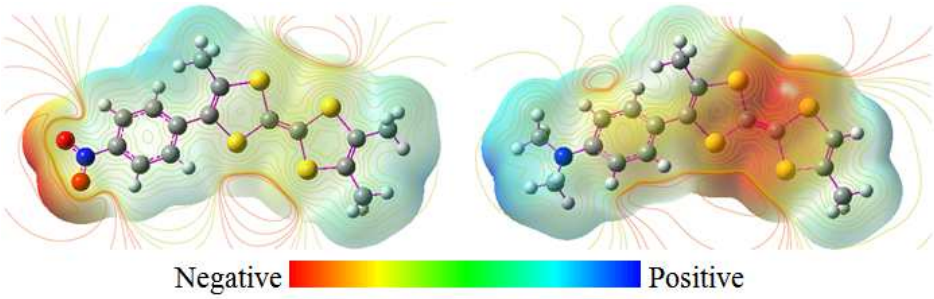

Global reactivity descriptors

The understanding of chemical reactivity and site selectivity of the molecular systems has been effectively handled by the conceptual density functional theory (DFT) [27]. Chemical potential, global hardness, global softness, electronegativity and electrophilicity are global reactivity descriptors, highly successful in predicting global chemical reactivity trends. Fukui functions (FF) and local softness are extensively applied to probe the local reactivity and site selectivity. The formal definitions of all these descriptors and working equations for their computation have been described [25-27]. Various applications of both global and local reactivity descriptors in the context of chemical reactivity and site selectivity have been reviewed in detail [28]. Parr et al. introduced the concept of Electrophilicity (ω) as a global reactivity index similar to the chemical hardness and chemical potential [28]. This reactivity index measures the stabilization in energy when the system acquires an additional electronic charge ΔN from the environment. The electrophilicity is defined as: ($\omega = \mu^2 / 2\eta$), $\mu \approx -(I+A)/2$ and $\eta \approx (I-A)/2$ are the electronic chemical potential and the chemical hardness of the ground state of atoms and molecules, respectively, approximated in terms of the vertical ionization potential (I) and electron affinity (A). The electrophilicity is a descriptor of reactivity that allows a quantitative classification of the global electrophilic nature of a molecule within a relative scale [29].

Table 4: Energetic parameters of TTF-donor substituted molecules (2-4)

Compounds	E_{HOMO} (eV)	E_{LUMO} (eV)	ΔE_{gap} (eV)	I (eV)	A (eV)
2b	-4.730	-2.560	2.169	4.730	2.560
2c	-4.776	-2.585	2.191	4.776	2.585
3b	-4.275	-0.734	3.541	4.275	0.734
3c	-4.315	-0.761	3.554	4.315	0.761
4b	-4.225	-0.689	3.536	4.225	0.689
4c	-4.254	-0.711	3.543	4.254	0.711

Figure 3. Highest occupied molecular orbitals and lowest unoccupied molecular orbitals of compounds (2b) and (4c)

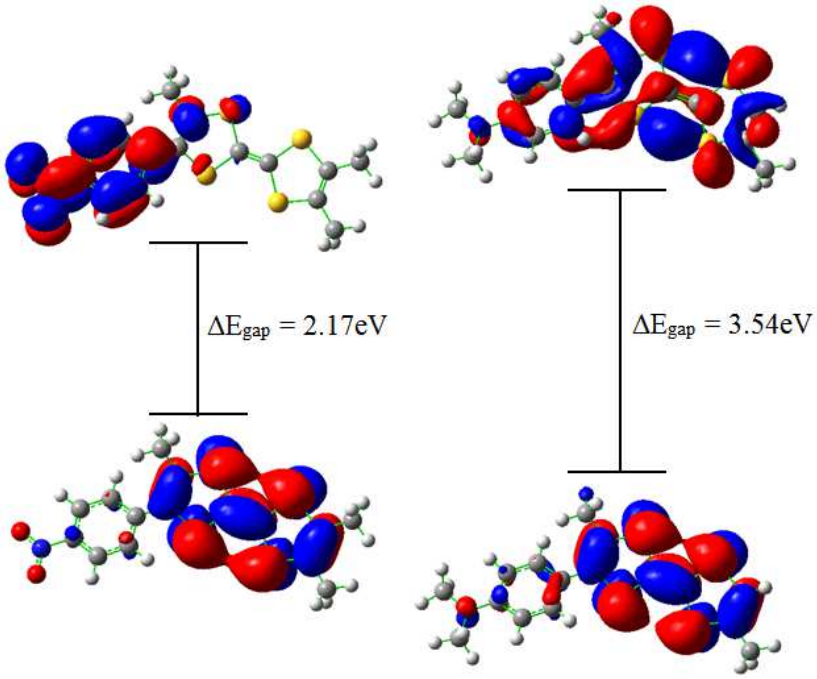

Table 5: Ouantum chemical descriptors of TTF-donor substituted molecules (2-4)

Compounds	μ(eV)	x(eV)	η(eV)	S(eV)	ω(eV)
2b	-3.645	3.645	1.085	0.461	6.124
2c	-3.680	3.680	1.096	0.456	6.181
3b	-2.505	2.505	1.771	0.282	1.772
3c	-2.538	2.538	1.777	0.281	1.813
4b	-2.457	2.457	1.768	0.283	1.708
4c	-2.483	2.483	1.772	0.282	1.740

As shown in table 4, the molecule (**2c**) is the most molecule has the ability to accept electrons (E_{HOMO} = -4,77eV) while (**4b**) has the highest HOMO energy (E_{HOMO} = -4,22eV) that allows him to be the best electron donor molecule. The high value of the energy gap indicates that the molecule shows high chemical stability, while a small HOMO-LUMO gap means small excitation energies to the manifold of excited states, table 4 shows that compound (**3c)** is the most stable. High ionization energy indicates high stability and chemical inertness and small ionization energy indicates high reactivity of the atoms and molecules. Compound (**4b**) has the lowest ionization potential value (I = 4,22eV) which indicate that it is the best electron donor. The electronic affinity (A) is defined as the energy released when an electron is added to a neutral molecule. A molecule with high (A) values tend to take electrons easily. From Table 4 it is clear that Compound (**2c**) is the best reactive.

Local reactivity descriptors

Fukui Function [30-32] is one of the widely used local density functional descriptors to model chemical reactivity and site selectivity and is defined as the derivative of the electron density $\rho(\vec{r})$ with respect to the total number of electrons N in the system, at constant external potential $v(\vec{r})$ acting on an electron due to all the nuclei in the system

$$f(\vec{r}) = \left[\delta\mu / \delta v(\vec{r})\right]_N = \left[\partial\rho(\vec{r}) / \partial N\right]_{v(\vec{r})}$$

The condensed Fukui Function are calculated using the procedure proposed by Yang and Mortier [33], based on a finite difference method

$$f^+ = [q(N+1) - q(N)], \text{ for nucleophilic attak,}$$
$$f^- = [q(N) - q(N-1)], \text{ for electrophilic attak,}$$
$$f^0 = [q(N+1) - q(N-1)]/2, \text{ for radical attak.}$$

Where q(N) is the charge on kth atom for neutral molecule while q(N + 1) and q(N - 1) are the same for its anionic and cationic species, respectively. The value of descriptors calculated at B3LYP/6-31G(d,p) level using Mulliken charges on atoms in molecules are presented in Table 6,7 and 8.

Table 6: Values of the Fukui function considering NBO charges of the molecules (2b) and (2c)

	Compound (2b)				Compound (2c)		
Atom	f^+	f^-	f^0	**Atom**	f^+	f^-	f^0
1 C	-0.024	0.009	-0.008	1 C	-0.016	0.008	-0.004
2 C	0.003	0.007	0.005	2 C	-0.001	-0.006	-0.003
3 C	0.003	0.006	0.005	3 C	0.003	0.012	0.008
4 C	**0.029**	-0.001	**0.014**	4 C	**0.028**	0.000	**0.014**
5 C	0.006	0.007	0.007	5 C	0.009	0.007	0.008
6 C	-0.043	0.004	-0.019	6 C	-0.042	0.004	-0.019
7 S	-0.040	-0.158	-0.099	7 S	-0.045	-0.162	-0.103
8 S	-0.070	-0.152	-0.111	8 S	-0.082	-0.156	-0.119
9 S	-0.045	-0.162	-0.103	9 S	-0.043	-0.167	-0.105
10 S	-0.033	-0.161	-0.097	10 S	-0.030	-0.161	-0.096
11 C	-0.013	**0.018**	0.002	11 C	-0.016	**0.017**	0.001
12 C	-0.021	-0.005	-0.013	12 C	-0.020	-0.005	-0.012
13 C	-0.008	-0.009	-0.009	13 C	-0.009	-0.009	-0.009
14 C	-0.025	-0.008	-0.017	14 C	-0.025	-0.008	-0.017
15 H	-0.056	-0.003	-0.029	15 H	-0.054	-0.003	-0.029
16 C	-0.028	-0.008	-0.018	16 C	-0.027	-0.008	-0.018
17 H	-0.055	-0.012	-0.033	17 H	-0.055	-0.012	-0.034
18 C	0.020	-0.005	0.008	18 C	0.019	-0.005	0.007
19 H	-0.051	-0.024	-0.038	19 H	-0.052	-0.024	-0.038
20 H	-0.053	-0.025	-0.039	20 H	-0.053	-0.026	-0.039
21 N	-0.106	-0.015	-0.061	21 N	-0.106	-0.016	-0.061
22 O	-0.132	-0.025	-0.078	22 O	-0.133	-0.025	-0.079
23 O	-0.133	-0.023	-0.078	23 O	-0.133	-0.023	-0.078
24 C	0.004	0.008	0.006	24 C	0.004	0.008	0.006
25 H	-0.017	-0.033	-0.025	25 H	-0.018	-0.036	-0.027
26 H	-0.016	-0.029	-0.022	26 H	-0.009	-0.032	-0.020
27 H	-0.005	-0.033	-0.019	27 H	-0.014	-0.034	-0.024
28 C	0.004	0.008	0.006	28 C	0.015	0.005	0.010
29 H	-0.008	-0.033	-0.020	29 H	-0.033	-0.031	-0.032
30 H	-0.018	-0.030	-0.024	30 H	0.003	-0.031	-0.014
31 H	-0.016	-0.033	-0.024	31 H	-0.040	-0.024	-0.032
32 C	0.014	0.005	0.009	32 H	-0.026	-0.058	-0.042
33 H	-0.030	-0.030	-0.030				
34 H	0.004	-0.031	-0.013				
35 H	-0.041	-0.023	-0.032				

Local reactivity descriptors are used to decide relative reactivity of different atoms in the molecule. It is established that molecule tends to react where the value of descriptor is largest when attacked by soft reagent and where the value is smaller when attacked by hard reagent [34]. The use of descriptors for the site selectivity of the molecule for nucleophilic and electrophilic attack has been made. Parameters of local reactivity descriptors show that 4C is more reactive site for nucleophilic and free radical attacks and 11C for electrophilic attack in compounds (**2b**-**2c**), for compounds (**3b**-**3c)** the most reactive site for nucleophilic and free radical attacks is 1C and 2C for electrophilic attack, 4C represent the more reactive site for nucleophilic and free radical attacks and 11C for electrophilic attack in compounds (**4b**-**4c**).

Principal Component Analysis (PCA):

In this work, we auto scaled all calculated variables in order to compare them in the same scale. Afterwards, PCA (principal component analysis) was used to reduce the number of variables and select the most relevant ones, i.e. those responsible for the *p*-Aminophenyl tetrathiafulvalenes reactivity. After performing many tests, a good separation is obtained between more active and less active tetrathiafulvalenes compounds using ten variables: I, A, χ , η, s, μ , ω, E_{HOMO} , E_{LUMO} , ΔE_{gap} (see Table 4 and 5).

We can observe from PCA results that the first three principal components (PC1, PC2 and PC3) describe 99.99% of the overall variance as follows: PC1 = 81.91%, PC2 = 11.54% and PC3 = 6.54%. The score plot of the variances is a reliable representation of the spatial distribution of the points for the data set studied after explaining almost all of the variances by the first two PCs. The most informative score plot is presented in Figure 4 (PC1 versus PC2) and we can see that PC1 alone is responsible for the separation between more active (**2b**, **2c**) and less active compounds (**3b**, **3c, 4b** and **4c**) where PC1>0 for the more active compounds and PC1<0 for the less active ones. The same results follow in the case of global reactivity trend based on ω.

Table 7: Values of the Fukui function considering NBO charges of the molecules (3b) and (3c)

	Compound (3b)				Compound (3c)		
Atom	f^+	f^-	f^0	**Atom**	f^+	f^-	f^0
1 C	**0.045**	0.011	**0.028**	1 C	**0.049**	0.011	**0.030**
2 C	-0.023	**0.017**	-0.003	2 C	-0.025	**0.018**	-0.004
3 C	0.001	0.001	0.001	3 C	0.001	0.001	0.001
4 C	0.003	0.001	0.002	4 C	-0.001	0.001	0.001
5 C	0.003	0.007	0.006	5 C	-0.004	-0.004	-0.004
6 C	0.002	0.007	0.005	6 C	0.007	0.012	0.009
7 S	-0.099	-0.146	-0.122	7 S	-0.094	-0.144	-0.119
8 S	-0.108	-0.146	-0.127	8 S	-0.102	-0.148	-0.125
9 S	-0.171	-0.148	-0.160	9 S	-0.178	-0.149	-0.164
10 S	-0.165	-0.162	-0.164	10 S	-0.169	-0.165	-0.167
11 C	0.027	-0.011	0.008	11 C	0.028	-0.013	0.008
12 C	-0.033	0.006	-0.014	12 C	-0.035	0.006	-0.014
13 C	-0.007	-0.005	-0.006	13 C	-0.008	-0.005	-0.006
14 C	0.001	-0.001	-0.001	14 C	0.001	-0.001	0.001
15 H	-0.024	-0.009	-0.017	15 H	-0.026	-0.009	-0.018
16 C	-0.004	-0.001	-0.002	16 C	-0.003	-0.001	-0.002
17 H	-0.029	-0.015	-0.022	17 H	-0.031	-0.016	-0.023
18 C	-0.058	-0.055	-0.057	18 C	-0.061	-0.058	-0.060
19 H	-0.041	-0.029	-0.035	19 H	-0.043	-0.030	-0.036
20 H	-0.041	-0.030	-0.036	20 H	-0.043	-0.031	-0.037
21 C	0.019	0.007	0.013	21 C	0.020	0.007	0.013
22 H	-0.035	-0.034	-0.035	22 H	-0.037	-0.035	-0.036
23 H	-0.025	-0.031	-0.028	23 H	-0.026	-0.031	-0.028
24 H	-0.040	-0.022	-0.031	24 H	-0.042	-0.022	-0.032
25 C	0.009	0.007	0.008	25 C	0.008	0.007	0.007
26 H	-0.026	-0.027	-0.026	26 H	-0.023	-0.031	-0.027
27 H	-0.028	-0.031	-0.029	27 H	-0.030	-0.033	-0.032
28 H	-0.022	-0.030	-0.026	28 H	-0.025	-0.028	-0.027
29 C	0.008	0.007	0.008	29 N	-0.003	0.004	0.001
30 H	-0.022	-0.030	-0.026	30 H	-0.029	-0.030	-0.029
31 H	-0.028	-0.031	-0.029	31 H	-0.029	-0.029	-0.029
32 H	-0.025	-0.026	-0.026	32 H	-0.047	-0.054	-0.051
33 N	-0.003	0.004	0.001				
34 H	-0.028	-0.028	-0.028				
35 H	-0.028	-0.028	-0.028				

Table 8: Values of the Fukui function considering NBO charges of the molecules (4b) and (4c)

	Compound (4b)				Compound (4c)		
Atom	f^+	f^-	f^0	**Atom**	f^+	f^-	f^0
1 C	-0.002	-0.001	-0.002	1 C	-0.005	-0.001	-0.003
2 C	0.002	0.007	0.004	2 C	-0.007	-0.004	-0.004
3 C	0.001	0.007	0.004	3 C	0.017	0.012	0.008
4 C	**0.044**	0.013	**0.029**	4 C	**0.060**	0.013	**0.030**
5 C	-0.004	0.002	-0.001	5 C	-0.001	0.002	-0.001
6 C	-0.029	**0.016**	-0.006	6 C	-0.014	**0.017**	-0.007
7 S	-0.159	-0.141	-0.150	7 S	-0.303	-0.140	-0.152
8 S	-0.156	-0.160	-0.158	8 S	-0.320	-0.162	-0.160
9 S	-0.091	-0.139	-0.115	9 S	-0.229	-0.141	-0.114
10 S	-0.081	-0.139	-0.110	10 S	-0.216	-0.137	-0.108
11 C	0.030	-0.015	0.008	11 C	0.013	-0.018	0.006
12 C	-0.026	0.006	-0.010	12 C	-0.036	0.007	-0.018
13 C	-0.016	-0.005	-0.010	13 C	-0.007	-0.004	-0.004
14 C	0.030	-0.008	0.011	14 C	0.005	-0.009	0.002
15 H	-0.025	-0.010	-0.017	15 H	-0.039	-0.012	-0.019
16 C	0.011	-0.009	0.001	16 C	0.014	-0.009	0.007
17 H	-0.030	-0.015	-0.023	17 H	-0.046	-0.016	-0.023
18 C	-0.123	-0.017	-0.070	18 C	-0.137	-0.016	-0.069
19 H	-0.034	-0.028	-0.031	19 H	-0.066	-0.028	-0.033
20 H	-0.038	-0.029	-0.033	20 H	-0.066	-0.030	-0.033
21 C	0.022	0.015	0.019	21 N	0.026	-0.006	0.013
22 H	-0.014	-0.015	-0.015	22 C	0.014	0.007	0.007
23 H	-0.045	-0.024	-0.035	23 H	-0.060	-0.032	-0.030
24 H	-0.030	-0.025	-0.028	24 H	-0.050	-0.027	-0.025
25 C	0.020	0.007	0.013	25 H	-0.050	-0.030	-0.025
26 H	-0.036	-0.035	-0.035	26 C	0.028	0.007	0.014
27 H	-0.024	-0.030	-0.027	27 H	-0.072	-0.035	-0.036
28 H	-0.040	-0.021	-0.031	28 H	-0.055	-0.031	-0.027
29 C	0.008	0.007	0.007	29 H	-0.064	-0.022	-0.032
30 H	-0.023	-0.025	-0.025	30 H	-0.095	-0.052	-0.048
31 H	-0.025	-0.030	-0.028	31 C	0.037	0.016	0.018

32 H	-0.020	-0.029	-0.025	32 H	-0.069	-0.025	-0.034
33 C	0.006	0.007	0.007	33 H	-0.033	-0.016	-0.016
34 H	-0.019	-0.029	-0.024	34 H	-0.058	-0.026	-0.029
35 H	-0.025	-0.030	-0.028	35 C	0.037	0.016	0.019
36 H	-0.022	-0.026	-0.024	36 H	-0.028	-0.015	-0.014
37 N	0.031	-0.004	0.013	37 H	-0.070	-0.025	-0.035
38 C	0.021	0.015	0.018	38 H	-0.057	-0.026	-0.028
39 H	-0.014	-0.015	-0.014				
40 H	-0.032	-0.025	-0.028				
41 H	-0.043	-0.023	-0.033				

Figure 4. Score plot for TTF-donor substituted molecules (2-4) in gas phase

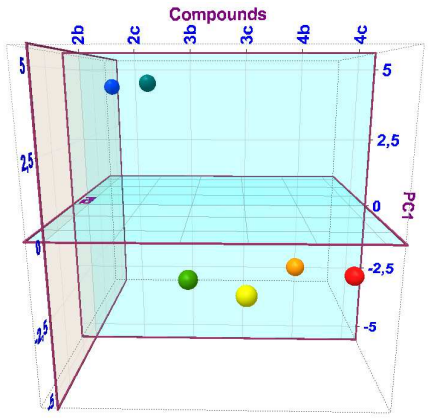

The loading vectors for the first two principal components (PC1 and PC2) are displayed in figure 5. We can see that more active compounds (PC1 > 0) can be obtained when we have higher A, I, S, χ, ω, values. In this way, some important features on the more active compounds can be observed.

Figure 5. Loading plot for the variables responsible for the classification of the TTF-donor substituted molecules studied

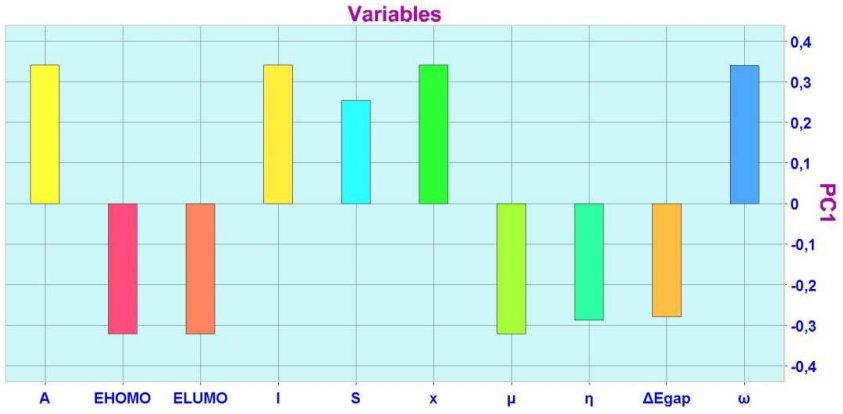

Hierarchical Cluster Analysis (HCA):

Figure 6 shows HCA analysis of the current study. The horizontal lines represent the compounds and the vertical lines the similarity values between pairs of compounds, a compound and a group of compounds and among groups of compounds. We can note that HCA results are very similar to those obtained with the PCA analysis, i.e. the compounds studied were grouped into two categories: more actives (compounds: **2b** and **2c**) and less active (compounds: **3b**, **3c, 4b** and **4c**).

Figure 6. Dendrogram obtained for TTF-donor substituted molecules studied

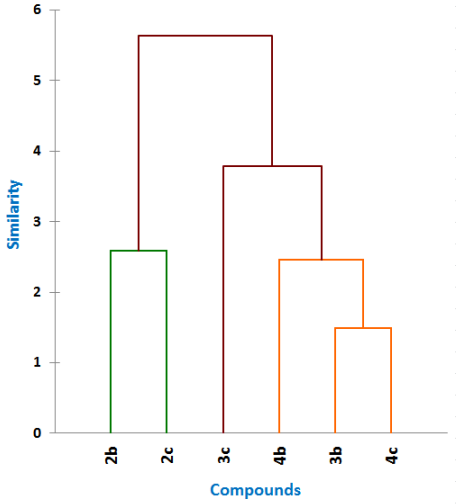

CONCLUSION

In conclusion, Based on the density functional theory B3LYP/6-31G(d,p) method, the global and local reactivity descriptors of the title compounds were performed and discussed. The descriptors obtained could provide more information and may contribute to a better understanding of the electronic structure of these compounds. From PCA results, Consistency between the results obtained through the reactivity descriptors and those that determined From PCA analysis. Finally we hope that these consequences will be of assistance in the quest of the experimental and theoretical evidence for the title compound in molecular bindings.

Acknowledgments
This work was generously supported by the (General Directorate for Scientific Research and Technological Development, DGRS-DT) and Algerian Ministry of Scientific Research.

REFERENCES

[1] J Becher; N Svenstrup. *Synthesis*, **1995**, 3, 215.
[2] MP Cava; NM Pollack; GA Dieterle. *J. Am. Chem. Soc*, **1973**, 95, 2558.
[3] F Wudl; GM Smith; EJ Hufnagel. *J. Chem. Soc. Chem. Comm*, **1970**, 1453.
[4] G Parr. *Annu. Rev. Phys. Chem*, **1983**, 34, 631.
[5] RG Parr; W Yang. Density Functional Theory of Atoms and Molecules; Oxford University Press: Oxford, UK, **1989.**
[6] H Chermette. *J. Comput. Chem*, **1999**, 20, 129.
[7] P Geerlings; F De Proft; W Langenaeker. *Chem. Rev*, **2003**, 103, 1793.
[8] P Hohenberg; W Kohn. *Phys. Rev. B*, **1964**, 136,864.
[9] W Kohn; LJ Sham. *Phys. Rev. A*, **1965**, 140, 1133.
[10] RG Parr; W Yang. *Ann. Rev. Phys. Chem*, **1995**, 46, 701.
[11] K Fukui; Y Yonezawa; H Shingu. *J. Chem, Phys*, **1952**, 20, 722.
[12] RG Parr; W Yang. *J. Am. Chem. Soc*, **1984**, 106, 4049.
[13] PW Ayers; M Levy. *Theor. Chem. Acc*, **2000**, 103, 353.
[14] MJ Frisch; GW Trucks; HB Schlegel; GE Scuseria; MA Robb; JR Cheeseman; G Scalmani; V Barone; B Mennucci; GA Petersson and al. Gaussian 09, Revision C.01; Gaussian Inc.: Wallingford, CT, USA, **2010**.
[15] HB Schlegel. *J. Comput. Chem*, **1982**, 3, 214.
[16] R Ditchfield; WJ Hehre; JA Pople, *J. Chem. Phys*, **1971**, 54, 724.
[17] R Dennington; T Keith and J Millam. GaussView, Version 5, Semichem Inc., Shawnee Mission, KS, **2009**.
[18] AD Becke. *J. Chem. Phys*, **1993**, 98, 5648.
[19] T Koopmans. *Physica*, **1993**, 1104.
[20] J F Lamère; I Malfant; A Sournia-Saquet; PG Lacroix; J M Fabre; L Kaboub; T Abbaz; AK Gouasmia; I Asselberghs and K Clays. *Chem. Mater*, **2007**, 19, 805.
[21] AT Bruni; VB Pereira. Quantum Chemistry and Chemometrics Applied to Conformational Analysis, Quantum Chemistry – Molecules for Innovations, Tomofumi Tada (Ed.), ISBN: 978-953-51-0372-1, InTech, **2012**, 15.
[22] NL Allinger. Molecular Structure Understanding Steric and Electronic Effects from Molecular Mechanics, A John Wiley & Sons, Inc. Publication, **2007**, 200.

[23] CS Tsai. Biomacromolecules Introduction to Structure, Function and Informatics, Wiley Publication, **2007**. 210.
[24] RM Mohareb; E El-Arabe; KA El-Sharkawy. *Sci. Pharm*, **2009**, 77, 355.
[25] RG Pearson. Chemical Hardness-Applications from Molecules to Solids, VCH-Wiley: Weinheim, **1997**.
[26] P Geerlings; F De Proft; W Langenaeker, *Chem. Rev*, **2003**, 103, 1793.
[27] PK Chattaraj. *J. Chem. Sci*, **2005**, 117.
[28] RG Parr; L V Szentpaly; S Liu, *J. Am. Chem. Soc*, **1999**, 121, 1922.
[29] PK Chattaraj; U Sarkar; DR Roy, *Chem. Rev*,**2006**, 106, 2065.
[30] RG Parr; W Yang, *J. Am. Chem. Soc*, **1984**, 106, 4049.
[31] K Fukui. *Science* **1987**, 218, 747.
[32] PW Ayers; M Levy. *Theor. Chem. Acc*, **2000**, 103, 353.
[33] W Yang; WJ Mortier. *J. Am. Chem. Soc*, **1986**, 108, 5708.
[34] J Sponer; P Hobza. *Int. J. Quantum Chem*. **1996**, 57, 959.